Autonomous Electrical Activity Induced By Cardiac Tissue Deformation In A Thermo-Electro-Mechanical Background ⋆

A. Collet * **T. Desaive.** * **P. C. Dauby** *

* *Thermodynamics of Irreversible Processes, University of Liège, Liège, Belgium (e-mail: A.Collet@ulg.ac.be).*

Abstract: In a healthy heart, the mechano-electric feedback (MEF) process acts as an intrinsic regulatory mechanism of the myocardium which allows the normal cardiac contraction by damping mechanical perturbations in order to generate a new healthy electromechanical situation. However, under certain conditions, the MEF can be a generator of dramatic arrhythmias by inducing local electrical depolarizations as a result of abnormal cardiac tissue deformations, *via* stretch-activated channels (SACs). Then, these perturbations can propagate in the whole heart and lead to global cardiac dysfunctions. In the present study, we examine the spatio-temporal behavior of the autonomous electrical activity induced by the MEF when the heart is subject to temperature variations. For instance, such a situation can occur during a therapeutic hypothermia. This technique is usually used to prevent neuronal injuries after a cardiac resuscitation. From this perspective, we introduce a one-dimensional time-dependent model containing all the key ingredients that allow accounting for excitation-contraction coupling, MEF and thermoelectric coupling. Our simulations show that an autonomous electrical activity can be induced by cardiac deformations, but only inside a certain temperature interval. In addition, in some cases, the autonomous electrical activity takes place in a periodic way like a pacemaker. We also highlight that some properties of the action potentials that are generated by the MEF, are significantly influenced by temperature. Moreover, in the situation where a pacemaker activity occurs, we also show that the period is heavily temperature-dependent.

Keywords: Biomedical systems, Electrical activity, Finite element analysis, Mechanical properties, Nonlinear models, Numerical simulation, Partial differential equations, Physiological models.

1. INTRODUCTION

In a healthy heart, cardiac beats, *i.e.* cardiac tissue contractions, are induced by a depolarization wave initiated by the *sino-atrial* (SA) node, which is located in the upper region of the right atrium. The SA node actually consists in a set of specialized cells which own the property to generate action potentials (APs) in a spontaneous and periodic way. After the SA node fires the electrical impulse, *i.e.* the AP, this signal spreads in a orderly fashion through the whole heart to allow normal cardiac tissue contraction and the resulting effective blood pumping. The contraction of cardiomyocytes due to electrical activity is known as the *excitation-contraction coupling* (ECC). When the SA node controls the cardiac contraction rhythm, the latter is called normal sinus rhythm. In turn, cardiac tissue mechanics also influences the electrical activity, *via stretch-activated channels* (SACs). This process is known as the *mechano-electric feedback* (MEF). In a healthy heart, the MEF acts as an intrinsic regulatory mechanism of the myocardium that allows the normal cardiac contraction by damping mechanical perturbations in order to generate a new healthy electromechanical situation. However, under certain conditions, the MEF can be a generator of dramatic arrhythmias by inducing local electrical depolarizations as a result of local abnormal cardiac tissue deformations. For instance, the MEF can induce atrial fibrillation (AF) (Nazir and Lab, 1996a,b; Ravelli, 2003; Kuijpers et al., 2007), one of the most common arrhythmias, characterized by rapid and irregular activation of the atrium, *e.g.* 400-600 pulses of the atrium muscular wall per minute in humans (Nattel, 2002). Instead of the SA node directing the cardiac electrical activity, many different electrical impulses are triggered in different regions of the atrium at once, following abnormal deformations, causing a very fast and chaotic rhythm.

In the present study, we qualitatively address the question of the role of thermal effects on the electromechanical behavior of the heart. More precisely, we examine the influence of temperature on the autonomous electrical activity, including pacemaker activity, induced by the MEF. Indeed, several studies have previously shown that the MEF can generate an autonomous electrical activity, sometimes in a periodic way like a pacemaker (Panfilov et al., 2005; Alvarez-Lacalle and Echebarria, 2009). In order to do this, we develop a one-dimensional time-dependent model taking into account three couplings: ECC, MEF and *thermoelectric coupling* (TEC), that is, the influence of tem-

⋆ We thank the Research Training Fund for Industry and Agriculture for its financial support as well as the French Community of Belgium (Actions de Recherches Concertées – Académie Wallonie-Europe).

perature on cardiac electrophysiology.
The clinical interest of our study is notably connected with *therapeutic hypothermia*, performed on a patient after a cardiac resuscitation for example. It consists in decreasing the body temperature in a significant way (typically 32^{o}C-34^{o}C) for 12-24 hours (Lee et al., 2011). The main objective of this procedure is to avoid neuronal injuries, *i.e.*, the therapeutic hypothermia has a *neuroprotective effect*.
The paper is organized in the following way. First, we introduce the model equations with the different assumptions in order to develop the computational model. Second, we briefly present the numerical methods used to develop the one-dimensional time-dependent model. Third, we show solutions obtained from numerical simulations and discuss them. Finally, we draw some conclusions.

2. ONE-DIMENSIONAL TIME-DEPENDENT MODEL

The main goal of the present study is to qualitatively and numerically investigate the influence of temperature on the properties of the pacemaker activity induced by the MEF by solving the equations of the system in a very simplified geometry. This model is not a quantitatively realistic description of the thermo-electro-mechanical behavior of the heart, but it can be considered as a numerical tool to examine from a qualitative point of view how the thermal effects influence the electromechanical behavior of the heart.

2.1 Modeling of cardiac electrical activity

Electrical activity at the cell level is due to ionic and capacitive currents across the cell membrane. Two main types of cell models are used to describe ionic flows through the membrane: qualitative and quantitative models. Qualitative models such as the Fitzhugh (FH) model (Fitzhugh, 1961), using a phenomenological approach, aim to globally describe the main features of the time course of the membrane potential V_m such as action potential duration (APD), action potential amplitude (APA) and refractoriness of cardiomyocytes. In turn, quantitative models, based on direct experimental observations derived from voltage clamp and patch clamp studies, generally include many Hodgkin–Huxley type equations to describe individual ionic currents that cross the cell membrane (Hodgkin and Huxley, 1952), resulting in a more accurate description of the time course of the membrane potential.
The total transmembrane current per unit area, I_m, can be split into two contributions as mentioned in the beginning of the present section. Mathematically, I_m can be written as (Hodgkin and Huxley, 1952; Keener and Sneyd, 2009):

$$I_m = C_m \frac{dV_m}{dt} + I_{ion} \,, \tag{1}$$

where C_m is the capacitance per unit area of the cell membrane and I_{ion} is the total ionic current per unit area, which can be described either by a qualitative or a quantitive model. When no external current is applied to a unique cell, not in contact with neighboring cells, then, the conservation of the total electric current implies that $I_m = 0$. Eq. (1) actually means that the current can be carried through the membrane either by charging the membrane capacitor or by movement of ions through the ionic channels in parallel with the capacitor (Hodgkin and Huxley, 1952). Given that the purpose of the present study is to examine a global behavior at a macroscopic level, accurate description of ionic currents is not needed and therefore, we have adopted a qualitative FH type model, called initially by Fitzhugh, the Boenhoeffer–van der Pol (BVP) model. It consists in a two-variable model. This model allows to reproduce key properties of the AP in a qualitative way. Moreover, a very interesting characteristic of this kind of simple model is that it can be studied not only numerically but also theoretically in order to predict its dynamical behavior for given parameter values. We discuss here the case of the FH model which consists in the following two ordinary differential equations (ODEs) (Keener and Sneyd, 2009):

$$\tau_m \frac{du}{dt} = f\,(u, v) \,, \tag{2}$$

$$\tau_m \frac{dv}{dt} = g\,(u, v) \,, \tag{3}$$

where the right hand sides of (2) and (3) are given by:

$$f\,(u, v) = k\,u\;(a - u)\;(u - 1) - v \,, \tag{4}$$

$$g\,(u, v) = \varepsilon\,(u)\;(b\,u - \gamma\,v - \delta) \,. \tag{5}$$

Note that the functions f and g described by (4) and (5) can be written in another way depending on the scaling of the constants and variables (Courtemanche et al., 1990). u and v are the two dependent variables of the FH system, the parameter a is a positive number representing the threshold value for excitation, while k, b, γ and δ are positive parameters that can modulate the dynamics of the system. Parameters τ_m and ε are, respectively, the membrane *time constant* classically introduced in the *cable equation* and the ratio between the two time scales, τ_u and τ_v, of the variables u and v (Keener and Sneyd, 2009). These times scales are such that $\tau_u << \tau_v$, which allows to assume $\varepsilon << 1$. From a physiological point of view, u represents the non-dimensional membrane potential, *i.e.*, the non-dimensional equivalent of V_m in (1). The variable t represents the time and (2) expresses the vanishing of I_m, while $f\,(u, v)$ represents the total ionic current. This ionic current depends on the variable v, known as the *gating variable* (non-dimensional) due to its original meaning in the HH model (Hodgkin and Huxley, 1952). This variable allows to account for accommodation and refractoriness (Fitzhugh, 1961) and influences the time evolution of the non-dimensional membrane potential u. Note that ε is a function of u in (5). This dependence has been introduced to better match the AP shape (Panfilov et al., 2005). In the present analysis, $\varepsilon = 0.025$ if $u > a$ and $\varepsilon = 0.75$ if $u \leq a$.
The model (2)-(5) can take account for two different dynamical regimes, namely, the *excitable regime* and the *oscillatory regime* (Keener and Sneyd, 2009). Given that cardiomyocytes are excitable and not self-oscillating, we have chosen in our study parameter values in such a way that the system (2)-(5) describes an excitable regime.
In order to describe the propagation of the cardiac electrical activity through the whole heart, we have to consider ohmic coupling between neighboring cells. In that situation, the Kirchhoff's current law leads to the well-known *monodomain model* (Keener and Sneyd, 2009) whose equation can be written:

$$\tau_m \frac{\partial u}{\partial t} = \lambda_m^2 \nabla^2 u + k\, u\, (a-u)\, (u-1) - v\,, \qquad (6)$$

where λ_m is the so-called *cable space constant* (Keener and Sneyd, 2009). In addition, by writting the monodomain equation as (6), we assume that cardiac tissue behaves like a homogeneous medium. In literature, (6) combined with (3) and (5) consist in the *Fitzhugh–Nagumo* (FHN) model (Keener and Sneyd, 2009; Bini et al., 2006). Moreover, it is interesting to note that using a qualitative model allows to save a huge computational cost in comparison with most quantitative models (Luo and Rudy, 1994; Noble et al., 1998) implying a large number of ODEs to solve.
Now, in order to take into account the stretch-activated currents across the SACs, *i.e.*, the currents due to the MEF, we have to introduce an additional term, and rewrite (6) as:

$$\tau_m \frac{\partial u}{\partial t} = \lambda_m^2 \nabla^2 u + k\, u\, (a-u)\, (u-1) - v - I_{sac}\,, \qquad (7)$$

where I_{sac} is given by (Panfilov et al., 2005; Alvarez-Lacalle and Echebarria, 2009):

$$I_{sac} = g_{sac}\, (F-1)\, (u - E_{sac})\, \Theta\,(F-1)\,. \qquad (8)$$

In (8), g_{sac} and E_{sac} are the non-dimensional maximal conductance and non-dimensional reversal potential of the SACs. $F = \frac{\partial x}{\partial X}$ where x and X are the spatial coordinates in the deformed and undeformed configurations, respectively (further explained in the next section). As for Θ, it is the Heaviside function. As a result, there is no additional currents when there is no stretching in the cardiac fiber ($I_{sac} = 0$ when $F \leq 1$).

2.2 Temperature dependence of cardiac electrophysiology

The influence of temperature on electrophysiology has been extensively studied for many years by using experimental approaches (Collins and Rojas, 1982; Sitsapesan et al., 1991) as well as modeling works (Fitzhugh and Cole, 1964; Fitzhugh, 1966; Bini et al., 2006). In the present study, two different influences of temperature on cardiac electrophysiology are taken into account, as suggested by Fitzhugh (Fitzhugh, 1966).
First, the gating kinetics of ion channels is assumed to be temperature dependent, *via* temperature-dependent rates for the conformational transitions of the subunits constituting the ion channels. By using a FH type model to describe cardiac electrical activity at a cell level, this dependence is taken into account by multiplying the right hand side of (5) by the following nonlinear temperature-dependent function (Fitzhugh, 1966; Bini et al., 2006):

$$\varphi\,(T) = Q_{10}^{\left(\frac{T-T_0}{10}\right)}\,, \qquad (9)$$

where T is the absolute temperature, T_0 is a reference temperature and Q_{10} represents the well-known 10-degree temperature coefficient which measures the change of rates due to a temperature increase of ten degrees. Actually, this coefficient can be linked to the Arrhenius activation energy which allows a more physical description of temperature effects on rates. In this study, we have chosen $T_0 = 33$°C because the target temperature of the therapeutic hypothermia is between 32°C and 34°C (Lee et al., 2011).
The second thermoelectric effect taken into account is the temperature dependence of ionic conductances. To model this influence, $k\, u\, (a-u)\, (u-1) - v - I_{sac}$, in the right hand side of (7), is multiplied by the following linear temperature-dependent function (Fitzhugh, 1966):

$$\eta\,(T) = A\, [(1 + B\, (T - T_0)]\,, \qquad (10)$$

where A and B are constants. A is actually a scale factor that has been historically introduced in order to update the ionic conductances values initially measured by Hodgkin and Huxley (Hodgkin and Huxley, 1952) following more accurate measures and B determines the rate of change of conductance with temperature (Fitzhugh, 1966; Bini et al., 2006).

2.3 Mechanical behavior of cardiac tissue

To describe the mechanical behavior of cardiac tissue, we need to solve the conservation of linear momentum and choose a constitutive law to account for the intrinsic mechanical properties of cardiac tissue. Given that the cardiac tissue has both active and passive behaviors, we split the constitutive law into two parts as explained further in this section (Nash and Hunter, 2000; Panfilov et al., 2005; Alvarez-Lacalle and Echebarria, 2009).
Although we study a one-dimensional case, we introduce cardiac mechanical equations in a more general way (three-dimensional case). The reduction of the equations to a one-dimensional configuration is trivial.
Assume that X^M and x^m ($M = 1, 2, 3$ and $m = 1, 2, 3$) represent two systems of coordinates relative to the undeformed and deformed configurations, respectively. Covariant base vectors $\mathbf{G_M}$, relative to the X^M-coordinate system, are chosen orthogonal and aligned with certain structural features of the material. Indeed, $\mathbf{G}_1$ is identified with the muscle fiber direction and, $\mathbf{G}_2$ and $\mathbf{G}_3$ are both perpendicular to $\mathbf{G}_1$ and between them. As for the covariant base vectors $\mathbf{g}_m$, which are relative to the x^m-coordinate system, they are generally not orthogonal anymore due to the deformation. Given that we solve the equations in order to obtain a one-dimensional dependence of the computed variables, we can choose to work with Cartesian coordinates for both undeformed and deformed configurations.
The passive behavior of cardiac tissue has been modeled by considering the cardiac tissue as a quasi-incompressible isotropic hyperelastic material. Therefore, for such a material, the components of the passive part of the second Piola–Kirchhoff (PK2) stress tensor $\mathbf{S}$ can be directly derived from a strain energy density function W in the following way (Malvern, 1969):

$$S_p^{MN} = 2\, \frac{\partial W}{\partial C_{MN}} - p\, C^{MN}\,, \qquad (11)$$

where S_p^{MN} and C_{MN} are the contravariant components of the passive part of the PK2 stress tensor and the covariant components of the right Cauchy–Green deformation tensor $\mathbf{C}$, respectively. As for p, it represents the hydrostatic pressure in the deformed configuration. Under the assumption of isotropy and quasi-incompressibility, W is a function of the first and second invariants of $\mathbf{C}$, namely I_1 and I_2. In addition, assuming that the cardiac tissue behaves like a hyperelastic material, a Mooney–Rivlin type model can

be used. Therefore, one has $W = c_1\ (I_1 - 3) + c_2\ (I_2 - 3)$ where c_1 and c_2 are constant material-dependent parameters (Panfilov et al., 2005; Alvarez-Lacalle and Echebarria, 2009).
In order to account for the active behavior of cardiac tissue, namely ECC, active stress components S_a^{MN} are linearly superimposed to the passive ones (Nash and Hunter, 2000; Panfilov et al., 2005; Alvarez-Lacalle and Echebarria, 2009) and assumed to act in the muscle fiber direction (aligned with the X^1-coordinate) (Nash and Hunter, 2000). The total stress components are consequently given by:

$$S^{MN} = S_p^{MN}\left(C_{MN}\right) + S_a^{MN}\left(C_{MN}, T_a\right)\,, \tag{12}$$

where the second term of the right hand side of (12) is given by (Nash and Hunter, 2000; Panfilov et al., 2005; Alvarez-Lacalle and Echebarria, 2009):

$$S_a^{MN}\left(C_{MN}, T_a\right) = T_a\, C^{11}\, \delta_1^{\,M}\, \delta_1^{\,N}\,. \tag{13}$$

In literature, the variable T_a is called the *active tension* and represents the active stresses generated by the sarcomeric units due to the electrical activation in cardiomyocytes. In our study, T_a is assumed to depend directly on the membrane potential with a time delay. As mentioned in Alvarez-Lacalle and Echebarria (2009), the generation of the active tension from the raise in the membrane potential is a rather strong simplification of the intracellular calcium dynamics, but it allows to take into account the basic delay between the initial fast inward currents and the final actin-myosin interactions resulting in the contraction. The time evolution of T_a is assumed to be governed by the following ODE:

$$\tau_m\, \frac{dT_a}{dt} = \varepsilon\left(u\right)\ \left(k_{T_a}\, u - T_a\right)\,, \tag{14}$$

where k_{T_a} is a parameter which controls the rate of active tension in cardiomyocytes and ε is the same small parameter as that introduced in (5).
Neglecting both body forces in the cardiac tissue and the inertial term, the conservation of the linear momentum can be written in terms of the PK2 stress tensor in the following way (Malvern, 1969):

$$\frac{\partial}{\partial X^M}\left(S^{MN}\, F_N^i\right) = 0\,, \tag{15}$$

where $F_N^i = \frac{\partial x^i}{\partial X^N}$ are the mixed components of the matrix accounting for the gradient deformation tensor $\mathbf{F}$.

3. NUMERICAL METHOD

The model introduced above has been numerically implemented by using the *COMSOL Multiphysics*® environment which uses the finite element method (FEM). The one-dimensional cardiac fiber of length L is modeled by a rectangular solving domain, $\Omega = [0, L] \times [0, l]$, with a ratio $L/l >> 1$, where l represents the width in the perpendicular direction (X^2) to the cardiac fiber direction (X^1). Note that only the cardiac fiber direction is relevant from a physical point of view. In order to mimic a one-dimensional study case with our two-dimensional solving domain Ω, the boundary and initial conditions have to be choosen in such a way that the results are X^2-independent, *i.e.*, all computed variables are homogeneous with regards to the X^2-coordinate.

3.1 Boundary and initial conditions

In order to fix the left and right boundaries of the cardiac fiber, we have applied a no-displacement condition on the left and right boundaries, labelled $\partial\Omega_1$ and $\partial\Omega_3$, respectively. Mathematically, we can write:

$$\text{on } \partial\Omega_1 \cup \partial\Omega_3 : \mathbf{x} = \mathbf{X}\,. \tag{16}$$

In addition, it has been assumed that the cardiac fiber is surrounded by an electrical insulator. Consequently, we have applied a no-flux boundary condition for the membrane potential u as follows:

$$\text{on } \partial\Omega_1 \cup \partial\Omega_2 \cup \partial\Omega_3 \cup \partial\Omega_4 : \mathbf{n} \cdot \left(\nabla\, u\right) = 0\,, \tag{17}$$

where $\mathbf{n}$ is the outward unit normal to the considered boundary and ∇ is the gradient operator; $\partial\Omega_2$ and $\partial\Omega_4$ are the labels relative to the "upper" and the "lower" boundaries of the solving domain, respectively. Moreover, in order to prevent rigid body motions in the X^2-direction, we have introduced an additional displacement constraint:

$$\text{on } \partial\Omega_2 \cup \partial\Omega_4 : x^2 = X^2\,. \tag{18}$$

With regards to the initial conditions, we have imposed a spatial distribution for u such as $u = 0$ in the whole cardiac fiber (*i.e.*, in the whole solving domain) excluding a small region, defined as $(L/2) - \epsilon^\star \leq X^1 \leq (L/2) + \epsilon^\star$, wherein $u = u_0$, where u_0 is a scalar value that represents the initial depolarization and $\epsilon^\star$ represents a very small value in comparison with L ($\epsilon^\star << L$). In addition, we have assumed that the cardiac fiber is initially undeformed. Mathematically, these conditions write, respectively:

$$\begin{aligned}\text{in } \Omega :\ u\left(\mathbf{X}, t_0\right) = u_0 \quad & \left[\Theta\left\{X^1 - \left(\frac{L}{2} - \epsilon^\star\right)\right\}\right. \\ & \left. -\Theta\left\{X^1 - \left(\frac{L}{2} + \epsilon^\star\right)\right\}\right]\,,\end{aligned} \tag{19}$$

$$\text{in } \Omega :\ \mathbf{x}\left(t_0\right) = \mathbf{X}\left(t_0\right)\,, \tag{20}$$

with t_0 that represents the initial time of the study.
In order to examine the role played by the temperature on the electromechanical behavior of the heart, we have performed several numerical simulations by changing the temperature value, all the other parameter values being identical in all simulations and given in Table 1.

4. SIMULATIONS AND DISCUSSION OF THE RESULTS

In order to characterize the influence of temperature on the pacemaker activity induced by cardiac tissue deformations, *via* the MEF, we have observed the spatio-temporal behavior of the membrane potential and represented space-time plots of this quantity.
First, the role of the MEF is illustrated in Fig. 1, which describes the behavior of the system when this effect is not taken into account (we have fixed $g_{sac} = 0$). The initial depolarization applied to the center of the fiber generates a local AP that then propagates in both directions in a

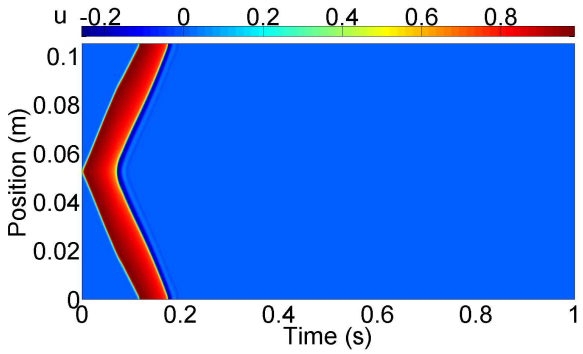

Fig. 1. Spatio-temporal behavior of the membrane potential u when the influence of the cardiac tissue deformations is not taken into account.

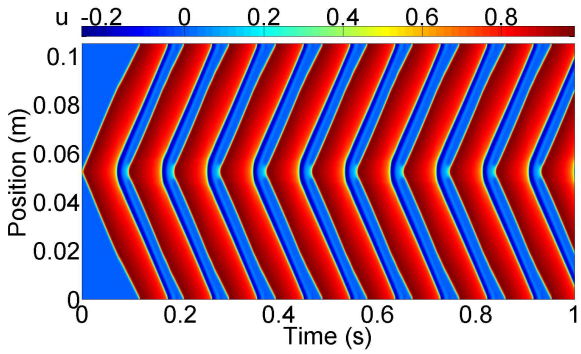

Fig. 2. Spatio-temporal behavior of the membrane potential u when the influence of the cardiac tissue deformations is taken into account *via* the MEF.

symmetric way (given that the electrical properties are homogeneous in the whole solving domain). As a result of this propagation, the fiber is deformed *via* the ECC but the electrical consequences of these deformations is absent as the MEF is not considered in this simulation. The electrical activity vanishes when the AP reaches the boundaries of the fiber.

In turn, in the situation where the MEF is incorporated in the model, the behavior is completely different (Fig. 2). In this case, the deformations of the fiber generate additional currents where there is a local stretching. In this way, an autonomous electrical activity can be triggered. This activity can occur in a periodic way and an endlessly sustainable fashion. That is the reason for which this activity is described as a pacemaker. Now, we can examine the effect of temperature on the mechanism highlighted in Fig. 2. In this perspective, we have plotted in Fig. 3 the time behavior of the membrane potential in a particular spatial position in the cardiac fiber, at the four fifths from one of the two boundaries, during a moderate hypothermia ($T = 35^o$C) and an acute hyperthermia ($T = 43^o$C). Fig. 3 shows that a temperature increase induces a significantly decrease of the APD. Moreover, we can also observe (Fig. 4) that the period of the pacemaker activity (*i.e.*, the interval between two successive maxima of the membrane potential) notably drops when the temperature is raised. Finally, we have also observed that the autonomous electrical activity occurs only inside a certain temperature interval. With the set of parameters listed in Table 1, this interval goes from 29^{o}C to 50.5^{o}C. Obviously, these values

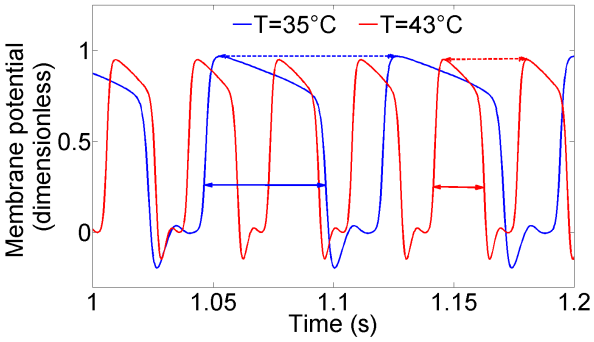

Fig. 3. APD (double full-line arrow) and period of the pacemaker activity (double dashed-line arrow) as functions of temperature.

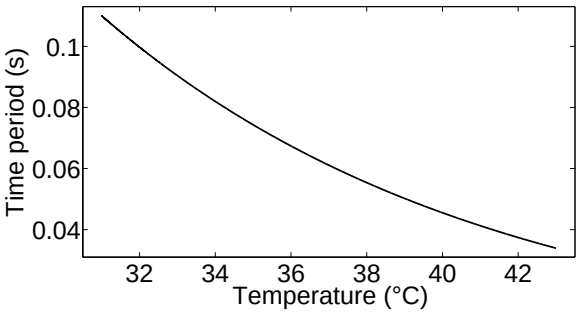

Fig. 4. Period of the pacemaker as a function of temperature.

Table 1. Parameters of the model (Fitzhugh, 1966; Panfilov et al., 2005; Keener and Sneyd, 2009; Alvarez-Lacalle and Echebarria, 2009). Parameters without units are non-dimensional.

Parameter	τ_m (s)	λ_m (m)	u_0	a	k
Value	$8.4\,10^{-3}$	$0.15\,10^{-2}$	0.9	0.05	16

Parameter	b	δ	γ	k_{T_a} (Pa)	g_{sac}
Value	16	0	1	$45\,10^3$	0.45

Parameter	E_{sac}	Q_{10}	A	B (1/^{o}C)	c_1 (Pa)
Value	1.2	3	1.14	0.06	$2\,10^3$

Parameter	c_2 (Pa)	L (m)	l (m)	p (Pa)	T_0 (^{o}C)
Value	$6\,10^3$	0.105	0.003	0	33

are not completely physiological but given that our study is generic and not species-specific oriented, it is not really surprising. In the case of a more species-oriented modeling, an autonomous electrical activity would also be induced by cardiac tissue deformations only inside a certain temperature interval, whose precise boundaries would be fixed by the model.

5. CONCLUSION

We have developed a one-dimensional time-dependent thermo-electro-mechanical model of a cardiac fiber which allows to describe ECC, MEF and TEC. Our model must be considered as a numerical tool allowing to characterize the qualitative effect of temperature on the electromechan-

ical behavior of the heart.

We have shown that the autonomous electrical activity, induced by cardiac tissue deformations *via* the MEF, takes place only inside a given interval of temperature. Furthermore, we have also found that for temperature values inside this interval but far from the boundaries, the tissue deformations generate an autonomous electrical activity in a periodic way (Fig. 2), *i.e.*, a pacemaker activity.

In addition, our numerical simulations have underlined that some properties of APs are heavily affected. For instance, we have shown that the APDs are dramatically shortened when the temperature increases.

Moreover, we have also highlighted that the period of the pacemaker activity notably drops when the temperature is raised.

It is important to note that this study consists in a first approach of the thermo-electro-mechanical cardiac process. In the present study, the cardiac excitation is modeled using a FH-type model and therefore, we do not expect to obtain a model that perfectly fits the electrophysiological properties.

In further modeling works, the cardiac excitation should be described by a more quantitative model so as to better match with the electrophysiological reality.

REFERENCES

Alvarez-Lacalle, E. and Echebarria, B. (2009). Global coupling in excitable media provides a simplified description of mechanoelectrical feedback in cardiac tissue. *Phys. Rev. E Stat. Nonlin. Soft. Matter. Phys.*, 79, 031921.

Bini, D., Cherubini, C., and Filippi, S. (2006). Heat transfer in Fitzhugh-Nagumo models. *Physical Review E*, 74, 041905.

Collins, C.A. and Rojas, E. (1982). Temperature dependence of the sodium channel gating kinetics in the node of Ranvier. *Q. J. Exp. Physiol.*, 67, 41–55.

Courtemanche, M., Skaggs, W., and Winfree, A.T. (1990). Stable three-dimensional action potential circulation in the Fitzhugh-Nagumo model. *Physica D: Nonlinear Phenomena*, 41, 173–182.

Fitzhugh, R. (1961). Impulses and physiological states in theoretical models of nerve membrane. *Biophys. J.*, 1, 445–466.

Fitzhugh, R. (1966). Theoretical effect of temperature on threshold in the Hodgkin-Huxley nerve model. *J. Gen. Physiol.*, 49, 989–1005.

Fitzhugh, R. and Cole, K.S. (1964). Theoretical potassium loss from squid axons as a function of temperature. *Biophysical Journal*, 4, 257–265.

Hodgkin, A.L. and Huxley, A.F. (1952). A quantitative description of membrane current and its application to conduction and excitation in nerve. *J. Physiol.*, 117, 500–544.

Keener, J.P. and Sneyd, J. (2009). *Mathematical physiology*. Springer, New York.

Kuijpers, N.H., ten Eikelder, H.M., Bovendeerd, P.H., Verheule, S., Arts, T., and Hilbers, P.A. (2007). Mechano-electric feedback leads to conduction slowing and block in acutely dilated atria: a modeling study of cardiac electromechanics. *Am. J. Physiol. Heart Circ. Physiol.*, 292, H2832–H2853.

Lee, J.H., Suh, G.J., Kwon, W.Y., Kim, K.S., Rhee, J.E., Kim, M.A., and Park, M.H. (2011). Protective effects of therapeutic hypothermia in post-resuscitation myocardium. *Resuscitation*, 18, 18.

Luo, C.H. and Rudy, Y. (1994). A dynamic model of the cardiac ventricular action potential. i. simulations of ionic currents and concentration changes. *Circ. Res.*, 74, 1071–1096.

Malvern, L.E. (1969). *Introduction to the mechanics of a continuous medium*. Prentice-Hall International.

Nash, M. and Hunter, P. (2000). Computational mechanics of the heart. *J. Elasticity*, 61, 113–141.

Nattel, S. (2002). New ideas about atrial fibrillation 50 years on. *Nature*, 415, 219–226.

Nazir, S.A. and Lab, M.J. (1996a). Mechanoelectric feedback and atrial arrhythmias. *Cardiovasc. Res.*, 32, 52–61.

Nazir, S.A. and Lab, M.J. (1996b). Mechanoelectric feedback in the atrium of the isolated guinea-pig heart. *Cardiovasc. Res.*, 32, 112–119.

Noble, D., Varghese, A., Kohl, P., and Noble, P. (1998). Improved guinea-pig ventricular cell model incorporating a diadic space, ikr and iks, and length- and tension-dependent processes. *Can. J. Cardiol.*, 14, 123–134.

Panfilov, A.V., Keldermann, R.H., and Nash, M.P. (2005). Self-organized pacemakers in a coupled reaction-diffusion-mechanics system. *Phys. Rev. Lett.*, 95, 258104.

Ravelli, F. (2003). Mechano-electric feedback and atrial fibrillation. *Prog. Biophys. Mol. Biol.*, 82, 137–149.

Sitsapesan, R., Montgomery, R.A., MacLeod, K.T., and Williams, A.J. (1991). Sheep cardiac sarcoplasmic reticulum calcium-release channels: modification of conductance and gating by temperature. *J. Physiol.*, 434, 469–488.